Modeling and Control of Unbalanced Three-Phase Systems Containing PWM Converters

Cursino Brandão Jacobina, *Senior Member, IEEE*, Maurício Beltrão de Rossiter Corrêa, Ricardo Ferreira Pinheiro, Edison Roberto Cabral da Silva, *Senior Member, IEEE*, and Antonio Marcus Nogueira Lima, *Member, IEEE*

***Abstract*—This paper proposes two complex vector models to characterize unbalanced three-phase four-wire systems that contain pulsewidth-modulated voltage-source converters (PWM-VSCs). In the first case, the three-phase system is decomposed in orthogonal odq components. A complex vector model is then built from the dq and o components. In the second case, a complex vector model is introduced by decomposing the system in three single-phase systems. In both cases, an orthogonal, fictitious circuit is introduced to handle a single-phase system, such as the homopolar system or each one of the three single-phase systems that compose a three-phase four-wire system. From the vector models, two digital controllers, which employ two different reference frames, are proposed. Also, the use of the same gains for both controllers simplifies the equations of the controller in the stationary reference frame. As an example, current control in a PWM-VSC system is presented.**

***Index Terms*—Current control, four-wire systems, unbalanced systems.**

NOMENCLATURE

Vectors and Matrices

$\mathbf{v}^s_{123}, \mathbf{i}^s_{123}$	Converter voltage and current.
$\mathbf{e}^s_{123}$	Load-grid-dependent voltage.
$\mathbf{e}^s_{g123}$	Grid voltage.
$\mathbf{e}^s_{l123}$	Load-dependent voltage.
$\mathbf{i}^s_{l123}$	Load current.
$\mathbf{R}_{123}, \mathbf{L}_{123}$	Equivalent resistance and inductance.
$\mathbf{R}_{g123}, \mathbf{L}_{g123}$	Resistance and inductance of the grid.

Complex Vectors in the Arbitrary Reference Frame

$\mathbf{v}^a_{dq}, \mathbf{v}^a_{oDQ}, \mathbf{v}^a_{nDQ}$	Converter voltages.
$\mathbf{i}^a_{dq}, \mathbf{i}^a_{oDQ}, \mathbf{i}^a_{nDQ}$	Converter currents.
$\mathbf{e}^a_{dq}, \mathbf{e}^a_{oDQ}, \mathbf{e}^a_{nDQ}$	Load-grid dependent voltages
$\bar{\mathbf{i}}^a_{dq}, \bar{\mathbf{i}}^a_{oDQ}, \bar{\mathbf{i}}^a_{nDQ}$	Complex conjugate currents.
$\tilde{\varepsilon}^a_{dq}, \tilde{\varepsilon}^a_{o}, \tilde{\varepsilon}^a_{oDQ}, \tilde{\varepsilon}^a_{nDQ}$	Unbalancing voltage terms.

Paper IPCSD 01–048, presented at the 1999 Industry Applications Society Annual Meeting, Phoenix, AZ, October 3–7, and approved for publication in the IEEE TRANSACTIONS ON INDUSTRY APPLICATIONS by the Industrial Power Converter Committee of the IEEE Industry Applications Society. Manuscript submitted for review August 1, 1999 and released for publication August 25, 2001.

C. B. Jacobina, E. R. C. da Silva, and A. M. N. Lima are with the Laboratório de Eletrônica Industrial e Acionamento de Máquinas, Departamento de Engenharia Elétrica, Universidade Federal da Paraíba, 58109-970 Campina Grande, Brazil (e-mail: jacobina@dee.ufpb.br; edison@dee.ufpb.br; amnlima@dee.ufpb.br).

M. B. de Rossiter Corrêa is with the Laboratório de Eletrônica Industrial e Acionamento de Máquinas, Departamento de Engenharia Elétrica, Universidade Federal da Paraíba, 58109-970 Campina Grande, Brazil, and also with the Coordenação de Ensino Tecnológico, Centro Federal de Educacção Tecnológica de Alagoas, 57601-220 Palmeira dos Índios, Brazil (e-mail: mbeltrao@ufpb.br).

R. F. Pinheiro is with the the Laboratório de Eletrônica Industrial e Acionamento de Máquinas, Departamento de Engenharia Elétrica, Universidade Federal da Paraíba, 58109-970 Campina Grande, Brazil, and also with the Departamento de Engenharia de Computação e Automação, Universidade Federal do Rio Grande do Norte, 59078-970 Natal, Brazil (e-mail: ricpinh@ufrnet.br).

Publisher Item Identifier S 0093-9994(01)10085-X.

I. INTRODUCTION

IN THREE-PHASE electrical systems, current control is often necessary, e.g., for rectifier input current control and active power filter current control. In such systems, unbalance is a very common situation [1].

The hysteresis type of current control scheme is an attractive solution when continuous or very-high sampling rate measurements are possible [7]. The use of proportional–integral (PI) or proportional–integral–derivative (PID) controllers is generally preferable for digital implementation. In addition, the use of the synchronous reference frame based on a PI controller has been shown to provide good results, since it provides zero steady-state error [2]. However, if the system is unbalanced, a single-synchronous-reference-frame-based controller is not able to achieve zero steady-state error. In previous work, a scheme with two controllers that uses different reference frames has been proposed to manage this situation [8], [3], [4]. Reference [8] employs two different reference frames to control an unbalanced induction machine. In [4], the compensation of the unbalancing is achieved by adding a negative-sequence controller. In [3], two synchronous-frame-based controllers are proposed to control an unbalanced three-phase three-wire load.

This paper proposes two different types of vector-modeling techniques to characterize unbalanced three-phase four-wire systems. To handle single-phase subsystems, like the homopolar system or each one of the three single-phase systems that compose a three-phase four-wire system, a fictitious circuit is introduced. The vector models are used to design two digital vector controllers, one for the positive-sequence vector and another for the negative-sequence vector. These controllers can be implemented in either the synchronous reference frame or stationary reference frame. Simulation and experimental results are presented for an unbalanced three-phase system containing a pulsewidth-modulated voltage-source converter (PWM-VSC).

II. THREE-PHASE SYSTEM MODEL

Fig. 1 presents an unbalanced three-phase four-wire system. This system contains an *ac* grid (infinite bus, line, and step-down transformer that are represented by a three-phase source with series impedance), a parallel *ac* load (three-phase and single-phase), a PWM-VSC with series impedance, a

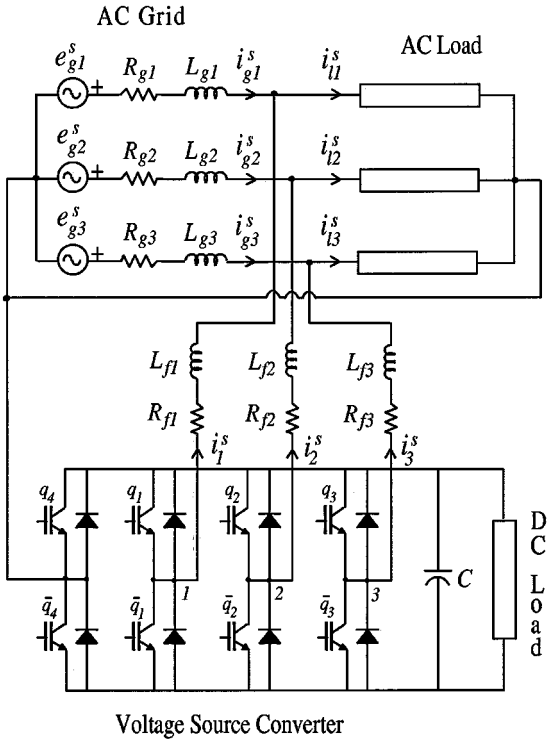

Fig. 1. Three-phase four-wire unbalanced system.

capacitor bank, and a *dc* load. Different interpretations can be provided for this configuration. For example, the PWM-VSC together with the capacitor bank (without dc load) can represent a shunt active power filter for the *ac* parallel load. Also, the PWM-VSC together with the capacitor bank can represent an adjustable and controlled voltage source for a *dc* load and the *ac* parallel load may represent the utility grid loading. In all cases, PWM-VSC currents are controlled in order either to accomplish the shunt filter objectives or to correct the input power factor of the *dc* voltage source.

A. Circuit Equations

The operation of the system given in Fig. 1 can be analyzed with the help of differential equations obtained from the electric power circuit. Kirchoff's laws applied to the circuit of Fig. 1 lead to

$$\mathbf{v}^s_{123} = \mathbf{R}_{123}\mathbf{i}^s_{123} + \mathbf{L}_{123}\frac{d\mathbf{i}^s_{123}}{dt} + \mathbf{e}^s_{123} \tag{1}$$

where

$$\mathbf{e}^s_{123} = \mathbf{e}^s_{g123} - \mathbf{e}^s_{l123}$$
$$\mathbf{e}^s_{l123} = \mathbf{R}_{g123}\mathbf{i}^s_{l123} + \mathbf{L}_{g123}\frac{d\mathbf{i}^s_{l123}}{dt}$$

and the superscript ^{s} indicates that the stationary reference frame is used.

The vectors appearing in (1) are defined as follows: $\mathbf{v}^s_{123} = [v^s_1\ v^s_2\ v^s_3]^T$ represents the voltages generated at the poles of the PWM-VSC, $\mathbf{i}^s_{123} = [i^s_1\ i^s_2\ i^s_3]^T$ represents the line currents flowing from the PWM-VSC, $\mathbf{e}^s_{g123} = [e^s_{g1}\ e^s_{g2}\ e^s_{g3}]^T$ represents the grid voltages, and $\mathbf{e}^s_{l123} = [e^s_{l1}\ e^s_{l2}\ e^s_{l3}]^T$ represents the voltages dependent of the load currents. The parameter matrices have the following structure:

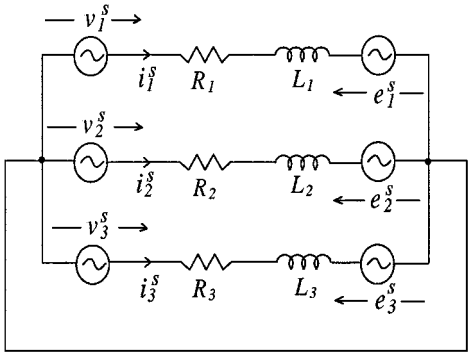

Fig. 2. Equivalent circuit for the three-phase four-wire unbalanced system.

$$\mathbf{R}_{123} = \begin{bmatrix} R_1 & 0 & 0 \\ 0 & R_2 & 0 \\ 0 & 0 & R_3 \end{bmatrix} \tag{2}$$

and

$$\mathbf{L}_{123} = \begin{bmatrix} L_1 & 0 & 0 \\ 0 & L_2 & 0 \\ 0 & 0 & L_3 \end{bmatrix} \tag{3}$$

with $R_1 = R_{g1} + R_{f1}, R_2 = R_{g2} + R_{f2}, R_3 = R_{g3} + R_{f3}$, $L_1 = L_{g1} + L_{f1}, L_2 = L_{g2} + L_{f2}$ and $L_3 = L_{g3} + L_{f3}$, where R_{g1} to R_{g3} and L_{g1} to L_{g3} are the resistance and the inductance of the grid, respectively, and where R_{f1} to R_{f3} and L_{f1} to L_{f3} are the resistance and the inductance of the converter filter, respectively. The matrices $\mathbf{R}_{g123}$ and $\mathbf{L}_{g123}$ are defined similarly to $\mathbf{R}_{123}$ and $\mathbf{L}_{123}$, with $R_1, R_2, R_3, L_1, L_2, L_3$ replaced by $R_{g1}, R_{g2}, R_{g3}, L_{g1}, L_{g2}$, and L_{g3}, respectively.

The model described by (1) can be represented by the series equivalent circuit given in Fig. 2.

The above equations have been written for an *ac* unbalanced load (passive or active) that is represented by its absorbed current. However, it is possible to extend this model to take into account the load explicitly, provided that a suitable voltage–current model is available. Also, by introducing a more elaborate model, the utility grid system (infinite bus, line, and step-down transformer) can be represented more realistically. However, from the feedback current control perspective, the voltage sources e^s_1 to e^s_3 (which depend on the specific type of load and type of grid connection) can be treated as unknown disturbances that must be compensated by the controller that defines the suitable control variables v^s_1 to v^s_3.

III. *odq* Vector Model

The conversion from the three-phase model given in (1) to an *odq* model requires the use of a coordinate transformation matrix. Among all possible choices, we adopted the 123—*odq* power conservative transformation [5] that is given by

$$\mathbf{x}^s_{123} = \mathbf{A}\mathbf{x}^s_{odq}$$

where $\mathbf{x}^s_{odq} = [x^s_o \ x^s_d \ x^s_q]^T$ and

$$\mathbf{A} = \sqrt{2/3}\begin{bmatrix} 1/\sqrt{2} & 1 & 0 \\ 1/\sqrt{2} & -1/2 & \sqrt{3}/2 \\ 1/\sqrt{2} & -1/2 & -\sqrt{3}/2 \end{bmatrix}.$$

Using this basic transforming equation for each term of (1), it follows that

$$v^s_o = R_o i^s_o + L_o \frac{di^s_o}{dt} + e^s_0 \tag{4}$$

where

$$e^s_0 = e^s_o + R_{od} i^s_d + R_{oq} i^s_q + L_{od}\frac{di^s_d}{dt} + L_{oq}\frac{di^s_q}{dt}$$

and

$$\begin{bmatrix} v^s_d & v^s_q \end{bmatrix}^T = \mathbf{R}_{dq}\mathbf{i}^s_{odq} + \mathbf{L}_{dq}\frac{d\mathbf{i}^s_{odq}}{dt} + \begin{bmatrix} e^s_d & e^s_q \end{bmatrix}^T \tag{5}$$

in which $\mathbf{i}^s_{odq} = [i^s_o \ i^s_d \ i^s_q]^T$ and

$$\mathbf{R}_{dq} = \begin{bmatrix} R_{od} & R_d & R_{dq} \\ R_{oq} & R_{dq} & R_q \end{bmatrix}$$
$$\mathbf{L}_{dq} = \begin{bmatrix} L_{od} & L_d & L_{dq} \\ L_{oq} & L_{dq} & L_q \end{bmatrix}$$

with $R_{od} = 1/(3\sqrt{2})(2R_1 - R_2 - R_3)$, $R_d = (1/6)(4R_1 + R_2 + R_3)$, $R_{dq} = 1/(2\sqrt{3})\,(R_3 - R_2)$, $R_{oq} = (1/\sqrt{6})(R_2 - R_3)$, $R_q = (1/2)(R_2 + R_3)$, $R_o = (R_1 + R_2 + R_3)/3$. The inductive terms are similarly defined to the resistive ones simply replacing R by L.

A. Complex Vector Model

The dq variables obtained by the previous procedure can be combined into complex vectors. These complex vectors given by

$$\mathbf{v}^s_{dq} = \frac{1}{\sqrt{2}}\left(v^s_d + jv^s_q\right) \tag{6}$$

$$\mathbf{i}^s_{dq} = \frac{1}{\sqrt{2}}\left(i^s_d + ji^s_q\right) \tag{7}$$

$$\mathbf{e}^s_{dq} = \frac{1}{\sqrt{2}}\left(e^s_d + je^s_q\right) \tag{8}$$

provide a more compact model representation. On the other hand, the complex vectors can be transformed to an arbitrary reference frame by introducing

$$\mathbf{v}^a_{dq} = e^{-j\delta_a}\mathbf{v}^s_{dq} \quad \mathbf{i}^a_{dq} = e^{-j\delta_a}\mathbf{i}^s_{dq} \quad \mathbf{e}^a_{dq} = e^{-j\delta_a}\mathbf{e}^s_{dq} \tag{9}$$

where $e^{-j\delta_a} = \cos\delta_a - j\sin\delta_a$ and the superscript ^{a} indicates that the reference frame is associated to the angular position δ_a $(d\delta_a/dt = \omega_a)$.

Now, from all these definitions, a complex vector model in arbitrary coordinates for (1) can be defined. Then, from (5) and using (6)–(9), the complex vector model is given by

$$\mathbf{v}^a_{dq} = \bar{R}_{dq}\mathbf{i}^a_{dq} + \bar{L}_{dq}\frac{d\mathbf{i}^a_{dq}}{dt} + j\omega_a\bar{L}_{dq}\mathbf{i}^a_{dq} + \mathbf{e}^a_{dq} + \tilde{\varepsilon}^a_{dq} + \tilde{\varepsilon}^a_o \tag{10}$$

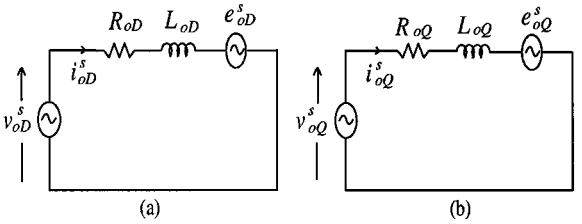

Fig. 3. Homopolar circuits for the vector model. (a) Actual single-phase circuit. (b) Fictitious single-phase circuit.

where

$$\tilde{\varepsilon}^a_{dq} = \tilde{R}_{dq}\bar{\mathbf{i}}^a_{dq} + \tilde{L}_{dq}\frac{d\bar{\mathbf{i}}^a_{dq}}{dt} + j\omega_a\tilde{L}_{dq}\bar{\mathbf{i}}^a_{dq}$$
$$\tilde{\varepsilon}^a_o = \tilde{R}_o e^{-j\delta_a} i^s_o + \tilde{L}_o e^{-j\delta_a}\frac{di^s_o}{dt}$$

and $\bar{\mathbf{i}}^a_{dq} = e^{-j\delta_a}\bar{\mathbf{i}}^s_{dq}$ in which $\bar{\mathbf{i}}^s_{dq} = (i^s_d - ji^s_q)/\sqrt{2}$ is the complex conjugate of $\mathbf{i}^s_{dq}$. Also, the parameters are given by $\bar{R}_{dq} = (R_d + R_q)/2$, $\tilde{R}_{dq} = (R_d - R_q + j2R_{dq})/2$, $\tilde{R}_o = (R_{od} + jR_{oq})/\sqrt{2}$, $\bar{L}_{dq} = (L_d + L_q)/2$, $\tilde{L}_{dq} = (L_d - L_q + j2L_{dq})/2$ and $\tilde{L}_o = (L_{od} + jL_{oq})/\sqrt{2}$.

It is worth noting that, if i^s_d and i^s_q are balanced sinusoidal two-phase variables, i.e., $i^s_d = I\cos(\omega_e t)$ and $i^s_q = I\sin(\omega_e t)$, then $\mathbf{i}^a_{dq}$ is a positive-sequence rotating vector (i.e., $\mathbf{i}^a_{dq} = (I/\sqrt{2})e^{j(\omega_e - \omega_a)t}$) and $\bar{\mathbf{i}}^a_{dq}$ is a negative-sequence rotating vector (i.e., $\bar{\mathbf{i}}^a_{dq} = (I/\sqrt{2})e^{-j(\omega_e + \omega_a)t}$).

If the system is balanced, then the parameter $\tilde{R}_{dq}, \tilde{L}_{dq}, \tilde{R}_o$, and $\tilde{L}_o$ are null and $\mathbf{e}^a_{dq}$ is a balanced vector (positive sequence). In this case, if $\mathbf{v}^a_{dq}$ is a positive-sequence vector, then $\mathbf{i}^a_{dq}$ is also a positive-sequence vector independently of $\tilde{\varepsilon}^a_{dq}$ and $\tilde{\varepsilon}^a_o$ that are both null. However, if $\tilde{R}_{dq}, \tilde{L}_{dq}, \tilde{R}_o$, and $\tilde{L}_o$ are not null, even if the vectors $\mathbf{v}^a_{dq}$ and $\mathbf{e}^a_{dq}$ are positive-sequence vectors, $\mathbf{i}^a_{dq}, \tilde{\varepsilon}^a_{dq}$ and $\tilde{\varepsilon}^a_o$ are positive- and negative-sequence vectors. The variables $\tilde{\varepsilon}^a_{dq}$ and $\tilde{\varepsilon}^a_o$ express the unbalancing of the RL part of the circuit.

From the feedback current control perspective, $\mathbf{v}^a_{dq}$ represents the manipulated control variable and $\mathbf{e}^a_{dq} + \tilde{\varepsilon}^a_{dq} + \tilde{\varepsilon}^a_o$ are the unknown unbalanced disturbances that must be compensated by the controller.

B. Homopolar Vector Model

The homopolar model is given by the scalar equation (4). Thus, it is not possible to define directly a complex vector model as was done for the dq components in the previous section. To overcome this difficulty, this paper introduces a method that leads to a complex vector model of the single-phase homopolar model obtained from DQ-axes components. Note that capital letters are used to distinguish this case from the case studied in previous sections.

In this method, the actual homopolar model corresponds to the oD single-phase homopolar circuit (Fig. 3(a)). Then, introducing $v^s_{oD} = v^s_o, i^s_{oD} = i^s_o$, and $e^s_{oD} = e^s_0$ and from (4), the actual oD model is obtained

$$v^s_{oD} = R_{oD} i^s_{oD} + L_{oD}\frac{di^s_{oD}}{dt} + e^s_{oD} \tag{11}$$

where $R_{oD} = R_o$ and $L_{oD} = L_o$. That circuit is shown in Fig. 3(a).

Now, a fictitious oQ model is defined as shown in Fig. 3(b)

$$v^s_{oQ} = R_{oQ} i^s_{oQ} + L_{oQ} \frac{di^s_{oQ}}{dt} + e^s_{oQ} \tag{12}$$

where R_{oQ} and L_{oQ} are the RL parameters and e^s_{oQ} is a voltage source. The fictitious circuit is similar to the oD circuit but it is associated to the oQ axis.

With the oD and oQ variables, it is possible to introduce the complex vectors

$$\mathbf{v}^s_{oDQ} = \frac{1}{\sqrt{2}} \left(v^s_{oD} + j v^s_{oQ} \right) \tag{13}$$

$$\mathbf{i}^s_{oDQ} = \frac{1}{\sqrt{2}} \left(i^s_{oD} + j i^s_{oQ} \right) \tag{14}$$

$$\mathbf{e}^s_{oDQ} = \frac{1}{\sqrt{2}} \left(e^s_{oD} + j e^s_{oQ} \right) \tag{15}$$

that can be represented in an arbitrary reference frame by introducing $\mathbf{v}^a_{oDQ} = e^{-j\delta} \mathbf{v}^s_{oDQ}$, $\mathbf{i}^a_{oDQ} = e^{-j\delta_a} \mathbf{i}^s_{oDQ}$, $\mathbf{e}^a_{oDQ} = e^{-j\delta_a} \mathbf{e}^s_{oDQ}$, as was done for the dq components in the previous section. Thus, the vector model for the homopolar circuit, in an arbitrary reference frame, is derived from (11) and (12) and is given by

$$\mathbf{v}^a_{oDQ} = \bar{R}^a_{oDQ} \mathbf{i}^a_{oDQ} + \bar{L}_{oDQ} \frac{d\mathbf{i}^a_{oDQ}}{dt} + j\omega_a \bar{L}_{oDQ} \mathbf{i}^a_{oDQ} + \mathbf{e}^a_{oDQ} + \tilde{\varepsilon}^a_{oDQ} \tag{16}$$

where

$$\tilde{\varepsilon}^a_{oDQ} = \tilde{R}_{oDQ} \bar{\mathbf{i}}^a_{oDQ} + \tilde{L}_{oDQ} \frac{d\bar{\mathbf{i}}^a_{oDQ}}{dt} + j\omega_a \tilde{L}_{oDQ} \bar{\mathbf{i}}^a_{oDQ}$$

$\bar{\mathbf{i}}^a_{oDQ} = e^{-j\delta_a} \bar{\mathbf{i}}^s_{oDQ}$ with $\bar{\mathbf{i}}^s_{oDQ} = (i^s_{oD} - j i^s_{oQ})/\sqrt{2}$ (i.e., the complex conjugate of $\mathbf{i}^s_{oDQ}$) and $\bar{R}_{oDQ} = (R_{oD} + R_{oQ})/2$, $\tilde{R}_{oDQ} = (R_{oD} - R_{oQ})/2$, $\bar{L}_{oDQ} = (L_{oD} + L_{oQ})/2$, $\tilde{L}_{oDQ} = (L_{oD} - L_{oQ})/2$.

The oQ model does not exist physically and was only introduced to generate the Q component and then to allow the definition of the homopolar vector model. Then, the Q components are obtained by solving numerically the model given by (12) on the microcomputer-based system simultaneously with the controller computation.

In the practical case, the parameters of the oD model are not completely known. Consequently, it is not possible to define a completely balanced DQ system so that the DQ system obtained is unbalanced. The disturbance term $\tilde{\varepsilon}^a_{oDQ}$ decreases when R_{oQ} and L_{oQ} tend to R_{oD} and L_{oD}, respectively. A negative-sequence disturbance also appears when $|e^s_{oQ}|$ and $\angle e^s_{oQ} - \pi/2$ are different from $|e^s_{oD}|$ and $\angle e^s_{oD}$, respectively. However, as will be shown, the controller is very robust and is able to compensate the disturbance term even if large differences occur between $R_{oQ}, L_{oQ}, |e^s_{oQ}|$ and $\angle e^s_{oQ} - \pi/2$ and $R_{oD}, L_{oD}, |e^s_{oD}|$ and $\angle e^s_{oD}$, respectively. Then, the unbalancing of the DQ model is not a critical issue.

Now, we have an unbalanced two-phase system composed of a oD real system and a simulated oQ system, which can be controlled by using vector control techniques, as it will be discussed in Section IV.

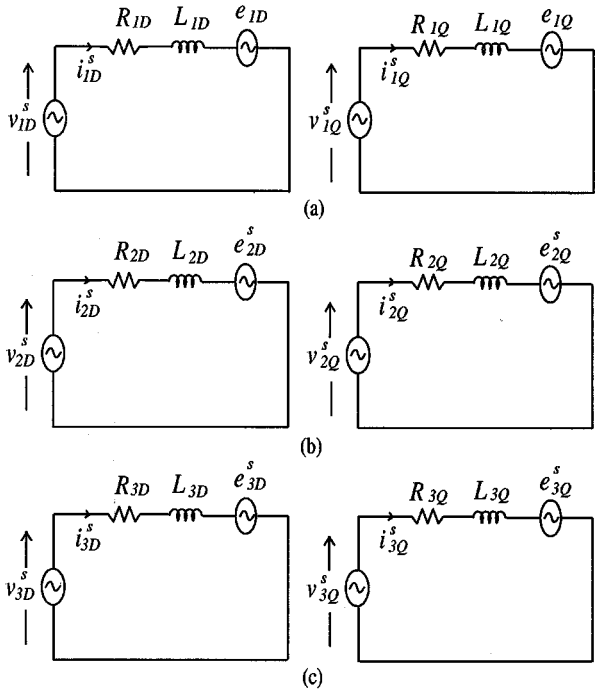

Fig. 4. Three single-phase circuits for the vector model. (a) Phase 1. (b) Phase 2. (c) Phase 3.

IV. Three-Phase Vector Model

The three-phase four-wire system shown in Fig. 2 can also be modeled by a set of three single-phase circuits. The technique of introducing the fictitious circuit can as well be employed with such a system. Fig. 4 shows the equivalent circuit from which the vector model for the system of Fig. 2 can be obtained.

For each one of the phases, a DQ model is defined. The D model corresponds to the real phase model and the Q model corresponds to the fictitious circuit. For a generic phase n ($n = 1, 2, 3$), the following equations can be written:

$$v^s_{nD} = R_{nD} i^s_{nD} + L_{nD} \frac{di^s_{nD}}{dt} + e^s_{nD} \tag{17}$$

$$v^s_{nQ} = R_{nQ} i^s_{nQ} + L_{nQ} \frac{di^s_{nQ}}{dt} + e^s_{nQ} \tag{18}$$

where $v^s_{nD} = v^s_n, R_{nD} = R_n, L_{nD} = L_n$, and $e^s_{nD} = e^s_n$, for $n = 1, 2, 3$.

Introducing the complex vector $\mathbf{v}^a_{nDQ} = e^{-j\delta_a}(v^s_{nD} + j v^s_{nQ})/\sqrt{2}$, $\mathbf{i}^a_{nDQ} = e^{-j\delta_a}(i^s_{nD} + j i^s_{nQ})/\sqrt{2}$, $\mathbf{e}^a_{nDQ} = e^{-j\delta_a}(e^s_{nD} + j e^s_{nQ})/\sqrt{2}$ and $\bar{\mathbf{i}}^a_{nDQ} = e^{-j\delta_a}(i^s_{nD} - j i^s_{nQ})/\sqrt{2}$, the vector model for a generic phase becomes

$$\mathbf{v}^a_{nDQ} = \bar{R}_{nDQ} \mathbf{i}^a_{nDQ} + \bar{L}_{nDQ} \frac{d\mathbf{i}^a_{nDQ}}{dt} + j\omega_a \bar{L}_{nDQ} \mathbf{i}^a_{nDQ} + \mathbf{e}^a_{nDQ} + \tilde{\varepsilon}^a_{nDQ} \tag{19}$$

where

$$\tilde{\varepsilon}^a_{nDQ} = \tilde{R}_{nDQ} \bar{\mathbf{i}}^a_{nDQ} + \tilde{L}_{nDQ} \frac{d\bar{\mathbf{i}}^a_{nDQ}}{dt} + j\omega_a \tilde{L}_{nDQ} \bar{\mathbf{i}}^a_{nDQ}$$

and $\bar{R}_{nDQ} = (R_{nD} + R_{nQ})/2, \tilde{R}_{nDQ} = (R_{nD} - R_{nQ})/2$, $\bar{L}_{nDQ} = (L_{nD} + L_{nQ})/2, \tilde{L}_{nDQ} = (L_{nD} - L_{nQ})/2$, for $n = 1, 2, 3$.

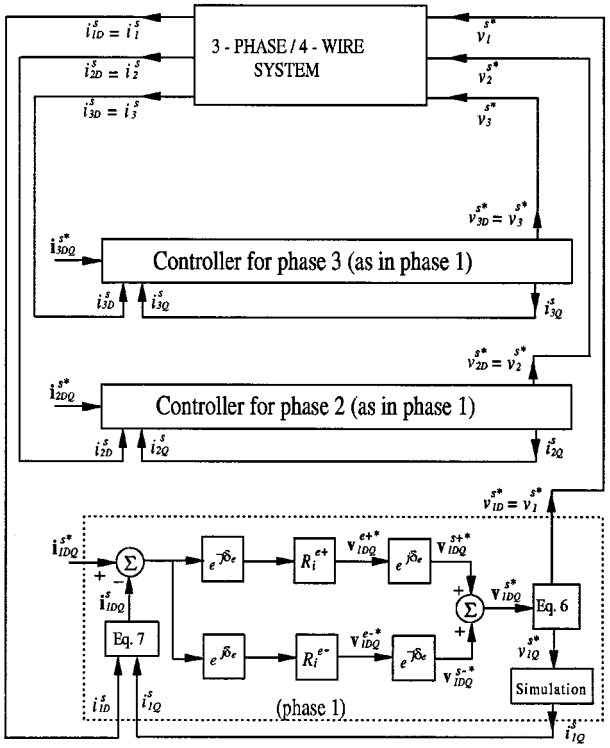

Fig. 5. Block diagram of the double synchronous current controller based on the three single-phase models in the synchronous frame.

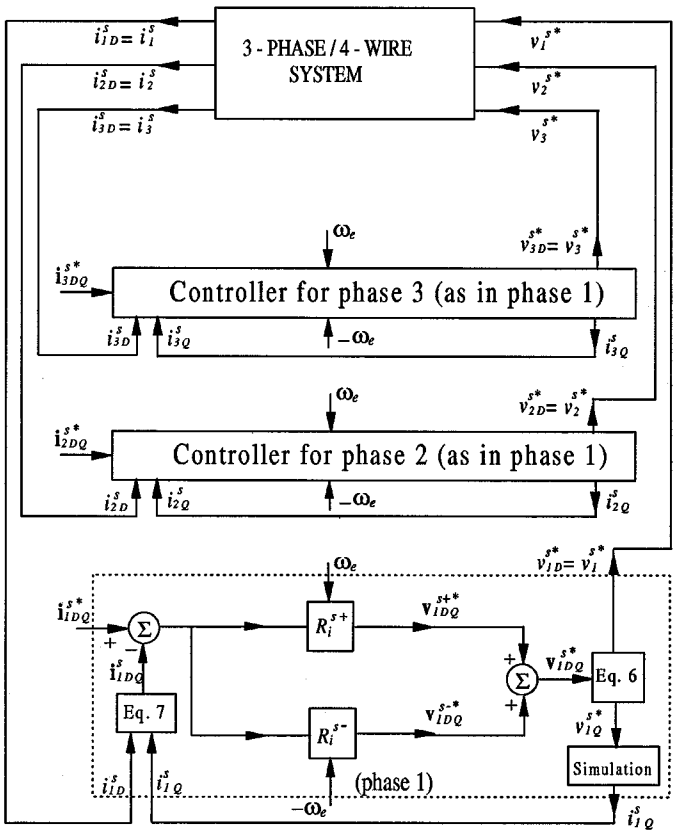

Fig. 6. Block diagram of the double synchronous current controller based on the three single-phase models in the stationary frame.

V. Control of the Unbalanced Three-Phase System

Let us consider again the system given in Fig. 2, where the three-phase load is fed by a VSI represented by the voltage sources v_1^s, v_2^s, and v_3^s. When the load is balanced and a PI controller is employed to control the load current, the use of a single synchronous reference frame has been proven to be the best choice. This happens because the disturbance terms (positive sequence) are transformed to *dc* quantities easily compensated by the controller itself. However, if the load is unbalanced, the use of a single synchronous reference frame ($\omega_a = \omega_e$) only solves the disturbance rejection for the positive-sequence term that rotates at the frequency $\omega_e - \omega_a = 0$. After the coordinate transformation is done, the disturbance becomes a *dc* component. Instead, the negative-sequence term becomes a component that rotates at $-2\omega_e$ and, consequently, cannot be compensated by a single controller.

The control concept used in this paper employs two different synchronous controllers. The positive-sequence synchronous controller rotates at $+\omega_e$ and is designed to compensate the positive-sequence term. The negative-sequence synchronous controller rotates at $-\omega_e$ and is designed to compensate the negative-sequence term. These two controllers (double controller) operate simultaneously, but their outputs are added.

There are two possibilities of using this control concept in this case.

- Case A uses a double synchronous controller to manage the dq components plus another for the homopolar term. For the homopolar term it is necessary to use the fictitious circuit, as presented in Section II-B.
- Case B uses a double synchronous controller for each phase as presented in Section III.

Figs. 5 and 6 present the block diagrams corresponding to the controllers for case B, which will be discussed in the next section. Fig. 5 corresponds to the synchronous frame version and Fig. 6 corresponds to the stationary frame version. Blocks $e^{j\delta_e}$ and $e^{-j\delta_e}$ perform the coordinate transformation from the stationary to the positive and negative synchronous reference frame, respectively. The superscripts $^{e+}$ and $^{s+}$ and $^{e-}$ and $^{s-}$ indicate the positive sequence and negative sequence, respectively. Block 3-PHASE/4-WIRE represents the system of Fig. 1 and the pulsewidth modulator control, and blocks R_i^{e+} and R_i^{e-} and R_i^{s+} and R_i^{s-} represent the controllers. In these figures, the D current is obtained from the system and the input system voltage is given by the D controller voltage. Instead, the Q current results from the simulation of the fictitious Q circuit, whose input is the Q controller voltage.

Figs. 7 and 8 present the block diagram corresponding to the controllers for case A. It is important to remark that, in this case, there are only two double synchronous controllers being used. However, there is a strong coupling between the dq and the homopolar components as can be observed from (10) and (16).

VI. Control Law

Assuming that PI controllers are used, the continuous-time state-space control law for the positive-sequence controller can be described by

$$\frac{d\mathbf{x}_{dqi}^{e+}}{dt} = k_i^+ \xi_{dq}^{e+} \tag{20}$$

$$\mathbf{v}_{dq}^{e+*} = \mathbf{x}_{dqi}^{e+} + k_p^+ \xi_{dq}^{e+} \tag{21}$$

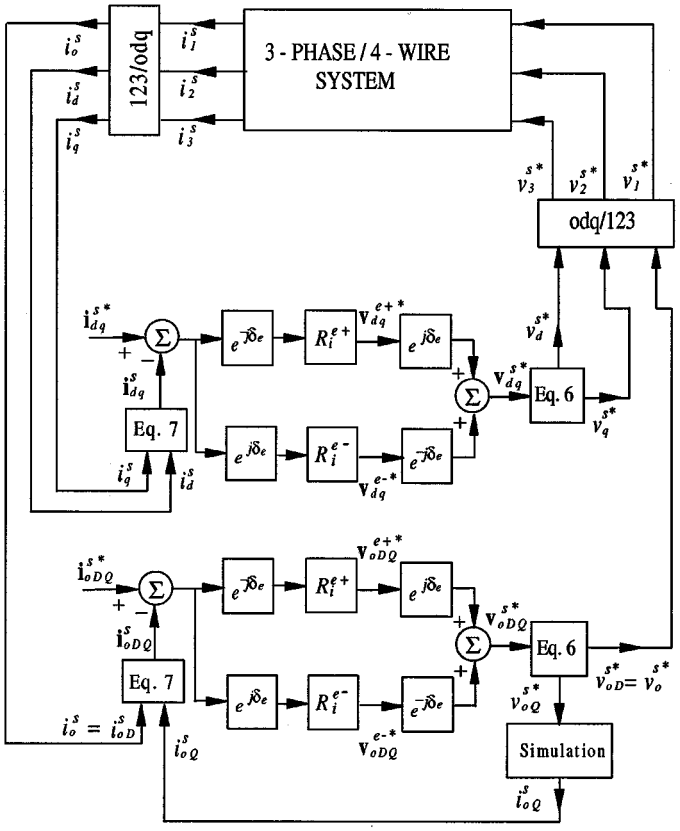

Fig. 7. Block diagram of the double synchronous current controller based on the odq model in the synchronous frame.

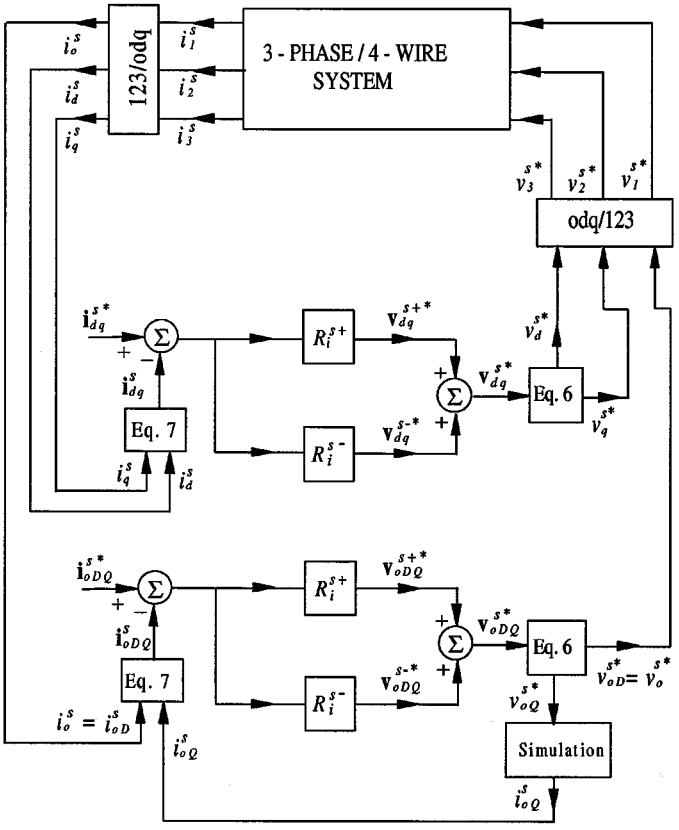

Fig. 8. Block diagram of the double synchronous current controller based on the odq model in the stationary frame.

where $\xi_{dq}^{e+} = \mathbf{i}_{dq}^{e+*} - \mathbf{i}_{dq}^{e+}$ is the current error and $\mathbf{v}_{dq}^{e+*}$ is the controller output (which is synthesized through the inverter and indicated by the superscript *). The parameters k_p^+ and k_i^+ are the gains of the controller. The control law for the negative-sequence controller has similar equations, but with the superscript $^+$ replaced by $^-$. The exact discrete-time version of the above control law, in terms of the d and q components, is given by

$$\mathbf{x}_{dqi}^{e+}(t) = \mathbf{x}_{dqi}^{e+}(t-h) + hk_i^+\xi_{dq}^{e+}(t-h) \tag{22}$$

$$\mathbf{v}_{dq}^{e+*}(t) = \mathbf{x}_{dqi}^{e+}(t) + k_p^+\xi_{dq}^{e+}(t) \tag{23}$$

where h is the sampling time.

In the block diagrams of Figs. 5 and 7, it is assumed that all the calculations are done in the synchronous reference frame, which explains the use of the coordinate transformers indicated in the diagram. However, this procedure can be avoided by emulating these synchronous controllers in the stationary reference frame, as presented in Figs. 6 and 8. The continuous-time version of the stationary controller that emulates the synchronous controller was proposed by Rowan and Kerkman [2].

From (20) and (21) by using the coordinate transformers $e^{j\delta_e}$ and $e^{-j\delta_e}$, the positive-sequence stationary continuous-time version can be obtained, that is,

$$\frac{d\mathbf{x}_{dqi}^{s+}}{dt} = k_i^+\xi_{dq}^s + j\omega_e\mathbf{x}_{dqi}^{s+} \tag{24}$$

$$\mathbf{v}_{dq}^{s+*} = \mathbf{x}_{dqi}^{s+} + k_p^+\xi_{dq}^s \tag{25}$$

where $\xi_{dq}^s = \mathbf{i}_{dq}^{s*} - \mathbf{i}_{dq}^s$. In this case, the exact discrete-time solution for the control law is given by

$$\mathbf{x}_{dqi}^{s+}(t) = e^{j\omega_e h}\mathbf{x}_{dqi}^{s+}(t-h) + jk_i^+\left(\frac{1-e^{j\omega_e h}}{\omega_e}\right)\xi_{dq}^s(t-h) \tag{26}$$

$$\mathbf{v}_{dq}^{s+*}(t) = \mathbf{x}_{dqi}^{s+}(t) + k_p^+\xi_{dq}^s(t). \tag{27}$$

These equations are more complex than those of the control law for the synchronous reference frame, especially when ω_e is time varying. When ω_e is time varying, matrices F and H for the discrete-time model ($\mathbf{x}(t) = F\mathbf{x}(t-h) + H\mathbf{u}(t-h)$) of the standard nth order continuous-time state-space model ($\dot{\mathbf{x}}(t) = A\mathbf{x}(t) + B\mathbf{u}(t)$) can also be calculated by

$$F = I + \sum_{k=1}^{\infty}\frac{A^k h^k}{k!} \quad \text{and} \quad H = \left(\sum_{k=1}^{\infty}\frac{A^{k-1}h^k}{k!}\right)B. \tag{28}$$

To obtain the discrete-time version of (24) and (25) by the use of (28), we first define $A = j\omega_e$ and $B = k_i^+$, and then decide at what order the power series should be truncated. If F and H are calculated with $k = 1$, the first-order discrete-time controller is given by

$$\mathbf{x}_{dqi}^{s+}(t) = \mathbf{x}_{dqi}^{s+}(t-h) + hk_i^+\xi_{dq}^s(t-h) + jh\omega_e\mathbf{x}_{dqi}^{s+}(t-h) \tag{29}$$

$$\mathbf{v}_{dq}^{s+*}(t) = \mathbf{x}_{dqi}^{s+}(t) + k_p^+\xi_{dq}^s(t). \tag{30}$$

When (29) is compared to (22), it can be seen that there is an additional term $jh\omega_e\mathbf{x}_{dqi}^{s+}(t-h)$ in the controller. Even with this additional term, this controller is simpler than the synchronous controller since it does not require any coordinate transformation. It is possible to improve the discrete-time representation by truncating F and H at $k = 2$ to obtain the second-order dis-

crete-time controller which, in terms of the d and q components, is given by

$$\mathbf{x}_{dqi}^{s+}(t) = \left(1 - h^2\,\omega_e^2/2\right)\mathbf{x}_{dqi}^{s+}(t-h) + hk_i^+\xi_{dq}^s(t-h) + jh\omega_e\mathbf{x}_{dqi}^s(t-h) + jh^2\omega_e k_i^+\xi_{dq}^s(t-h)/2. \quad (31)$$

As in the previous case, the expression to compute $\mathbf{v}_{dq}^{s+*}(t)$ is also given by (30). The negative-sequence stationary controller is obtained substituting ω_e by $-\omega_e$ in the previous equations.

As has been mentioned before, when ω_e is constant or when (28) is truncated at $k = 1$, the stationary frame controller is simpler than the synchronous frame controller because it does not require any coordinate transformation. However, when higher order approximation is necessary or when it is desired to take advantage of the high switching frequency capability of the converter, as proposed in [6], then the use of the synchronous frame controller can be preferable.

The use of same gains k_i and k_p for all controllers provides a simpler controller model when the stationary reference frame is employed. In fact, in this case the equations for the double-controller strategy are given by

$$\frac{d\mathbf{x}_{dqi}^{s+}}{dt} = j\omega_e\mathbf{x}_{dqi}^{s+} + k_i\xi_{dq}^s \quad (32)$$

$$\frac{d\mathbf{x}_{dqi}^{s-}}{dt} = -j\omega_e\mathbf{x}_{dqi}^{s-} + k_i\xi_{dq}^s \quad (33)$$

$$\mathbf{v}_{dq}^{s*} = \mathbf{x}_{dqi}^{s+} + \mathbf{x}_{dqi}^{s-} + 2k_p\xi_{dq}^s. \quad (34)$$

Now, introducing $\mathbf{x}_{dqi}^s = \mathbf{x}_{dqi}^{s+} + \mathbf{x}_{dqi}^{s-}$ and $\mathbf{x}_{dqi}^{s\prime} = j\omega_e(\mathbf{x}_{dqi}^{s+} - \mathbf{x}_{dqi}^{s-})$, the equations of the controller become

$$\frac{d\mathbf{x}_{dqi}^s}{dt} = 2k_i\xi_{dq}^s + \mathbf{x}_{dqi}^{s\prime} \quad (35)$$

$$\frac{d\mathbf{x}_{dqi}^{s\prime}}{dt} = -\omega_e^2\mathbf{x}_{dqi}^s \quad (36)$$

$$\mathbf{v}_{dq}^{s*} = \mathbf{x}_{dqi}^s + 2k_p\xi_{dq}^s. \quad (37)$$

This controller is slightly simpler than the controller given by (32) and (34) and the d-axis equations are decoupled from the q-axis equation. In this case, it is not necessary to simulate the q-axis model.

The discrete-time version of the simplified continuous-time control law given in (35)–(37) is

$$\mathbf{x}_{dqi}^s(t) = \cos(\omega_e h)\mathbf{x}_{dqi}^s(t-h) + \frac{1}{\omega_e}\sin(\omega_e h)\mathbf{x}_{dqi}^{s\prime}(t-h) + 2k_i\frac{1}{\omega_e}\sin(\omega_e h)\xi_{dq}^s(t-h) \quad (38)$$

$$\mathbf{x}_{dqi}^{s\prime}(t) = -\omega_e\sin(\omega_e h)\mathbf{x}_{dqi}^s(t-h) + \cos(\omega_e h)\mathbf{x}_{dqi}^{s\prime}(t-h) + 2k_i[\cos(\omega_e h) - 1]\xi_{dq}^s(t-h) \quad (39)$$

$$\mathbf{v}_{dq}^{s+*}(t) = \mathbf{x}_{dqi}^s(t) + k_p\xi_{dq}^s(t). \quad (40)$$

VII. Simulation Results

Figs. 9 and 10 show the converter current error obtained for the controller in Fig. 6, for the single synchronous controller (only the positive sequence synchronous controller) and for the standard scalar stationary controller (the d-axis component in (24) and (25) with $\omega_e = 0$). In this case, the system is a three-phase *RLE* load fed by an ideal voltage source and $h = 100\ \mu$s. The reference currents for phase 1 are given by $i_1^{s*} = I\cos(\omega_e t), 0 \le t < t_{\max}/2$, and

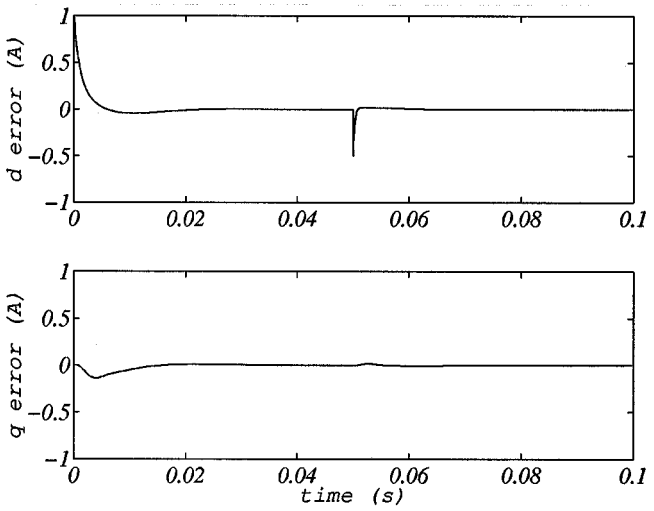

Fig. 9. d-axis and q-axis currents errors for the double synchronous controller.

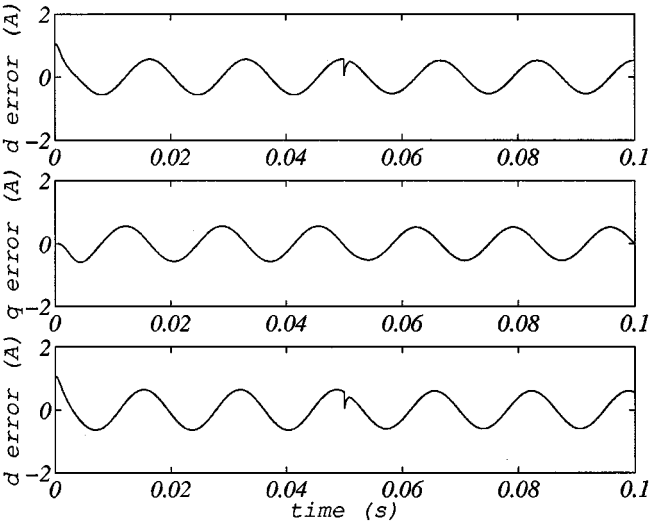

Fig. 10. d-axis and q-axis currents errors (top) for the single synchronous controller and d-axis current error (bottom) for the standard stationary controller.

$i_1^{s*} = (I/2)\cos(\omega_e t), t_{\max}/2 \le t \le t_{\max}$, where $I = 1$ A, $\omega_e = 120\pi$ rad/s, and $t_{\max} = 0.1$ s. The parameters of the Q fictitious model are $R_{nQ} = R_{nD}/2, L_{nQ} = 3L_{nD}, e_{nQ} = 0, i_{nQ}^{s*} = 0, k_i^- = k_i^+/2$ and $k_p^- = k_p^+/2$. These waveforms show that the errors observed with the single controller and with the standard stationary controller are no longer zero, however, the error with the double controllers tends to zero.

VIII. Experimental Results

The experimental setup is constituted by an unbalanced *ac* load being supplied by a voltage-source converter and controlled through a Pentium II 266-MHz equipped with dedicated plug-in boards with $h = 100\ \mu$s.

Fig. 11 shows the three-phase reference currents ($i_1^{s*} = i_{1D}^{s*}, i_2^{s*} = i_{2D}^{s*}$, and $i_3^{s*} = i_{3D}^{s*}$) and the actual three-phase currents, ($i_1^s = i_{1D}^s, i_2^s = i_{2D}^s$, and $i_3^s = i_{3D}^s$) superimposed when the double synchronous current controller in Fig. 5 is used. The unbalanced load has been implemented

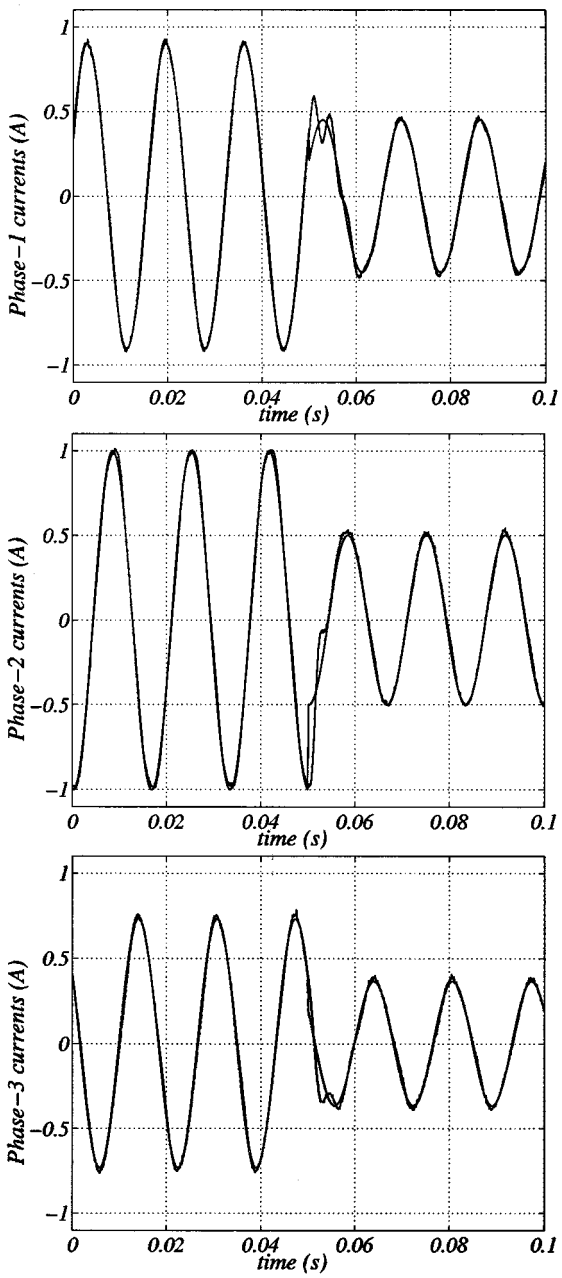

Fig. 11. Experimental reference and load currents obtained with the double synchronous controller (first test).

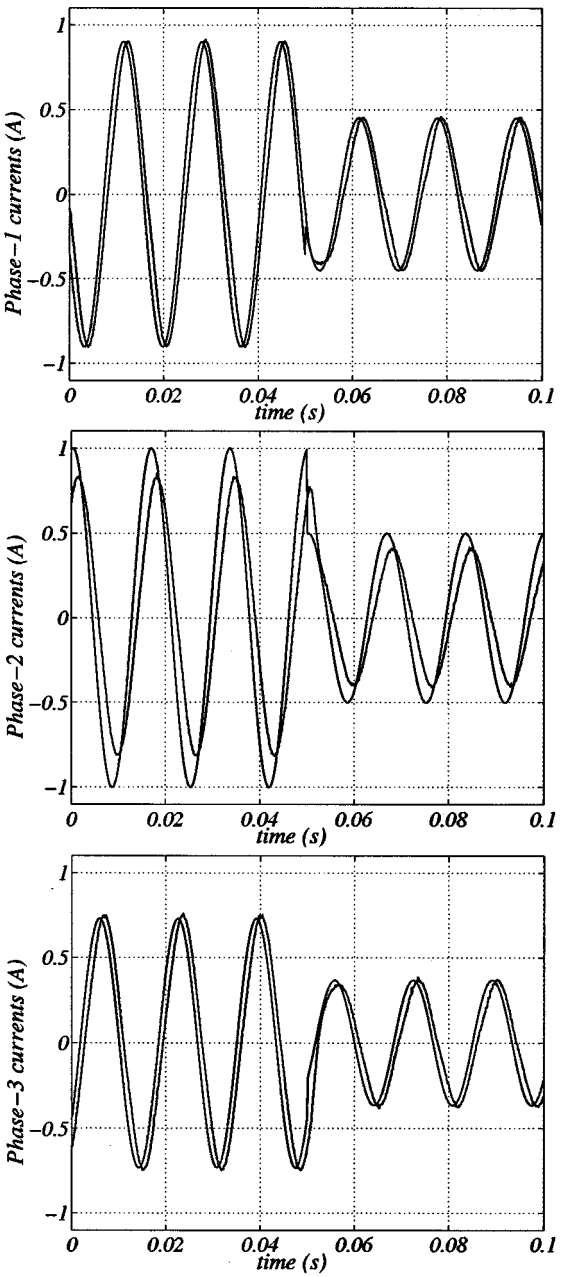

Fig. 12. Experimental reference and load currents phase currents obtained with the single synchronous controller (first test).

by using a three-phase induction machine. One resistor of 26 Ω has been connected in series with one of the machine windings, while one inductor of 23 mH has been added in series with another winding. The parameters of the motor is $R_s = 26.8\ \Omega$, $R'_r = 26.8\ \Omega$, $L_{\sigma s} = 23$ mH, $L'_{\sigma r} = 23$ mH, and $L_m = 0.498$ H. Note that the neutral of the load is connected to the fourth leg of the converter to obtain an unbalanced phase-neutral load. The reference currents are given by $i_1^{s*} = I_1 \cos(\omega_e t)$, $i_2^{s*} = I_2 \cos(\omega_e t - 2\pi/3)$, $i_3^{s*} = I_3 \cos(\omega_e t + 2\pi/3)$, $0 \leq t < t_{\max}/2$, and $i_1^{s*} = (I_1/2)\cos(\omega_e t)$, $i_2^{s*} = (I_2/2)\cos(\omega_e t - 2\pi/3)$, $i_3^{s*} = (I_3/2)\cos(\omega_e t + 2\pi/3)$, $t_{\max}/2 \leq t \leq t_{\max}$, where $I_1 = 0.9$ A, $I_2 = 1.0$ A, $I_3 = 0.73$ A, $\omega_e = 120\pi$ rad/s, and $t_{\max} = 0.1$ s. Note that the homopolar component exists since the instantaneous sum of the three load currents reference is not zero. Fig. 12 shows the corresponding results obtained when only the single synchronous positive sequence is used. These waveforms show that the actual currents track quite well the reference currents when the double synchronous current controller is used. However, the single controller presents a large steady-state current control error.

Fig. 13 shows the results of a second experimental test where the double synchronous controller is used to control another unbalanced load configuration. In this case, the load is composed of the machine employed in the first test with the resistor now connected in parallel with one of the machine windings. The neutral of the load is connected to the fourth leg of the converter. The reference currents are given by

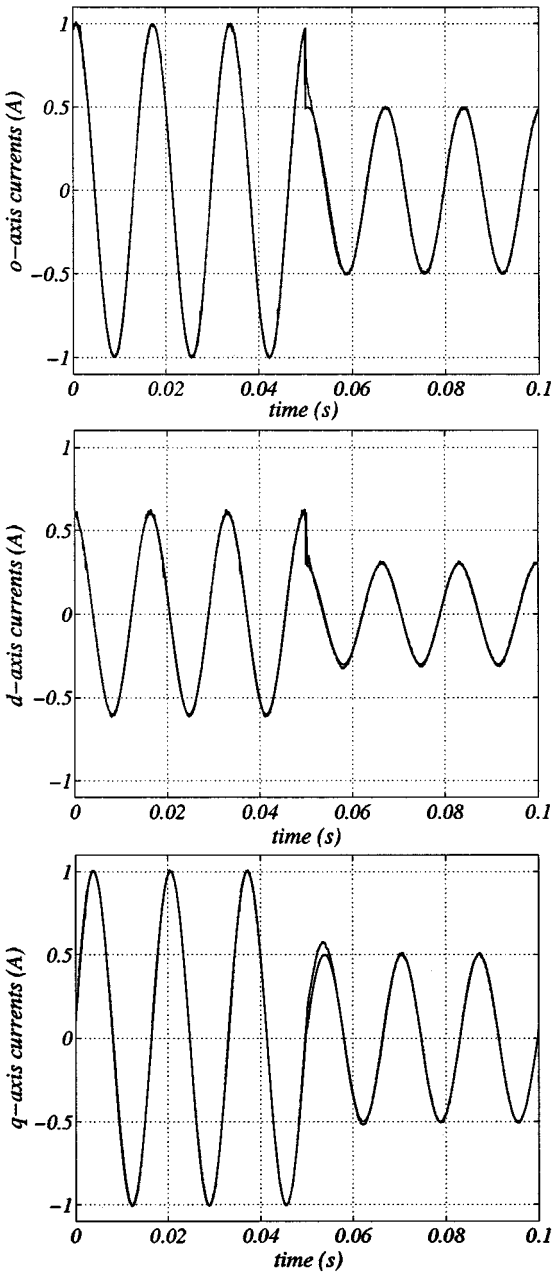

Fig. 13. Experimental reference and load odq currents obtained with the double synchronous controller (second test).

$i_o^{s*} = I\cos(\omega_e t - 36°), i_d^{s*} = 0.6I\cos(\omega_e t), i_q^{s*} = I\sin(\omega_e t)$ for $0 \le t < t_{\max}/2$, and $i_o^{s*} = (I/2)\cos(\omega_e t - 36°), i_d^{s*} = (0.6I/2)\cos(\omega_e t), i_q^{s*} = (I/2)\sin(\omega_e t)$ for $t_{\max}/2 \le t \le t_{\max}$, with $I = 1$ A, $\omega_e = 120\pi$ rad/s, and $t_{\max} = 0.1$ s. Again, it is worth noting that the use of the double synchronous current controller provides a very good behavior. Instead, the use of the single controller (whose test results are not presented here) leads to a large steady-state current error, similar to that found in Fig. 12.

IX. Conclusion

This paper has presented two different vector modeling approaches to characterize unbalanced three-phase four-wire systems. These techniques are useful to analyze three-phase electrical systems containing power converters and unbalanced loads. In both cases, an orthogonal, fictitious circuit was introduced to handle a single-phase system, such as the homopolar system or each one of the three single-phase systems that compose a three-phase four-wire system. The vector models have been used to define a current control strategy that uses two different controllers in the synchronous frame or in the stationary reference frame. In the stationary reference frame, the use of the same gains for both controllers simplifies the equations of the control law. Simulation and experimental results have demonstrated the correctness of the methodology and warrant the feasibility of the proposed techniques.

References

[1] J. W. Dixon, J. J. García, and L. Morán, "Control system for three-phase active power filter which simultaneously compensates power factor and unbalanced load," *IEEE Trans. Ind. Electron.*, vol. 42, pp. 636–641, Dec. 1995.

[2] T. M. Rowan and R. J. Kerkman, "A new synchronous current regulator and an analysis of a current-regulated PWM inverter," *IEEE Trans. Ind. Applicat.*, vol. 22, pp. 678–690, July/Aug. 1986.

[3] P. Hsu and M. Behnke, "A three-phase synchronous frame controller for unbalanced load," in *Proc. IEEE PESC'98*, 1998, pp. 1369–1374.

[4] H. S. Kim, H. S. Mok, G. H. Choe, D. S. Hyun, and S. Y. Choe, "Design of current controller for 3-phase PWM converter with unbalanced input voltage," in *Proc. IEEE PESC'98*, 1998, pp. 503–509.

[5] D. C. White and H. H. Woodson, *Electromechanical Energy Conversion*. New York: Wiley, 1959.

[6] C. B. Jacobina, A. M. N. Lima, and A. C. Oliveira, "Enhanced PWM voltage waveform and dead time compensation for AC drive systems," in *Proc. IEEE IECON'97*, 1997, pp. 694–697.

[7] P. Verdelho and G. D. Marques, "An active power filter and unbalanced current compensator," *IEEE Trans. Ind. Electron.*, vol. 44, pp. 321–328, June 1997.

[8] Y. Zhao and T. A. Lipo, "Modeling and control of a multi-phase induction machine with structural unbalance," *IEEE Trans. Energy Conversion*, vol. 11, pp. 570–584, Sept. 1995.

Cursino Brandão Jacobina (S'78–M'78–SM'98) was born in Correntes, Brazil, in 1955. He received the B.S. degree in electrical engineering from the Federal University of Paraíba, Campina Grande, Brazil, and the Diplôme d'Etudes Approfondies and the Ph.D. degree from the Institut National Polytechnique de Toulouse, Toulouse, France, in 1978, 1980, and 1983, respectively.

Since 1978, he has been with the Electrical Engineering Department, Federal University of Paraíba, where he is currently a Professor of Electrical Engineering. His research interests include electrical drives, power electronics, control systems, and system identification.

Maurício Beltrão de Rossiter Corrêa was born in Maceió, Brazil, in 1973. He received the Bachelor's and Master's degrees in electrical engineering in 1996 and 1997, respectively, from the Federal University of Paraíba, Campina Grande, Brazil, where he is currently working toward the Doctoral degree.

Since 1997, he has also been a faculty member of the Coordenaçâo de Ensino Tecnológico—Centro Federal de Educacção Tecnológica de Alagoas, Palmeira dos Índios, Brazil. His research interests include power electronics and electrical drives.

Ricardo Ferreira Pinheiro was born in Natal, Brazil, in 1956. He received the Bachelor's degree from the Federal University of Rio Grande do Norte, Natal, Brazil, and the Master's degree from the Federal Engeneering School of Itajubá, Brazil, in 1978 and 1980, respectively, both in electrical engineering. He is currently working toward the Doctoral degree in electrical engineering at the Federal University of Paraíba, Campina Grande, Brazil.

Since 1978, he has been with the Electrical Engineering Department, Federal University of Rio Grande do Norte, where he is currently a Professor of Electrical Engineering. His research interests include active filter drives and power electronics.

Edison Roberto Cabral da Silva (SM'95) was born in Pelotas, Brazil, in 1942. He received the B.C.E.E. degree from the Polytechnic School of Pernambuco, Recife, Brazil, the M.S.E.E. degree from the University of Rio de Janeiro, Rio de Janeiro, Brazil, and the D.Eng. degree from the University Paul Sabatier, Toulouse, France, in 1965, 1968, and 1972, respectively.

In 1967, he joined the staff of the Electrical Engineering Department, Federal University of Paraiba, Campina Grande, Brazil, where he is a Professor of Electrical Engineering and Director of the Research Laboratory on Industrial Electronics and Machine Drives. In 1990, he was with COPPE, Federal University of Rio de Janeiro and, from 1990 to 1991, he was with WEMPEC, University of Wisconsin, Madison, as a Visiting Professor. His current research work is in the areas of power electronics and motor drives. He was the General Chairman of the 1984 Joint Brazilian and Latin-American Conference on Automatic Control, sponsored by the Automatic Control Brazilian Society.

Dr. da Silva is currently a Member-at-Large of the Executive Board of the IEEE Industrial Applications Society.

Antonio Marcus Nogueira Lima (S'77–M'89) was born in Recife, Brazil, in 1958. He received the B.S. and M.S. degrees in electrical engineering from the Federal University of Paraíba, Campina Grande, Brazil, and the Ph.D. degree from the Institut National Polytechnique de Toulouse, Toulouse, France, in 1982, 1985, and 1989, respectively.

He was with the Escola Técnica Redentorista, Campina Grande, Brazil, from 1977 to 1982 and was a Project Engineer with Sul-América Philips, Recife, Brazil, from 1982 to 1983. Since September 1983, he has been with the Electrical Engineering Department, Federal University of Paraíba, where he is currently a Professor of Electrical Engineering. His research interests are in the fields of electrical machines and drives, power electronics, electronic instrumentation, control systems, and system identification.